Nafion/IL hybrid membranes with tuned nanostructure for enhanced CO_2 separation: effects of ionic liquid and water vapor

Zhongde Dai, [iD] †[a] Luca Ansaloni, [iD] †[a] Justin J. Ryan,[b] Richard J. Spontak [iD] [b,c] and Liyuan Deng [iD] *[a]

Polyelectrolytes have been reported to display gas permeation properties that can be of significant interest for CO_2 capture applications, especially when they are fully hydrated. In this work, hybrid membranes prepared by co-casting an ionic liquid (IL), 1-butyl-3-methylimidazolium tetrafluoroborate ([Bmim][BF_4]), with Nafion have been investigated for use in carbon capture. Gas permeabilities of different gaseous species have been measured for IL concentrations up to 40 wt%. Moreover, the effect of water vapor on gas permeation is examined with humidified CO_2/N_2 gas mixtures at various relative humidity (RH) levels. These experiments reveal that CO_2 permeability is greatly enhanced upon addition of the IL and in the presence of water in the gas stream, most likely due to the formation of IL nanochannels in the Nafion matrix. Small-angle X-ray scattering confirms changes in the nanostructure at different IL loading levels. Hybrid membranes containing 40 wt% [Bmim][BF_4] exhibit a mixed-gas CO_2 permeability of 390 Barrer with a corresponding CO_2/N_2 selectivity of ~30 at 100% RH, which is more than 3× that of the permeability measured from the same IL-containing membrane in the dry state and more than 200× higher than that of dry Nafion. Such improvements suggest the existence of a synergetic relationship between the IL and water vapor with regard to Nafion gas-transport properties, yielding superior separation performance with an enhanced gas flux compared to extruded Nafion membranes. These results represent a viable fabrication strategy for the production of thin Nafion-based membranes for CO_2 capture.

1. Introduction

Ionic liquids (ILs) are salts composed of organic cations and (in)organic anions typically with a melting point below 100 °C. Due to their unique physicochemical properties such as high CO_2 solubility and selectivity, low volatility and designer molecular structure to tune chemical/physical properties, ILs have been proposed as stand-alone materials for diverse applications such as green solvents for chemical reactions or syntheses, catalysts, electrolytes, and gas-separation solvents.[1,2] In particular, research efforts over the past decade have attempted to combine ILs with polymer membrane technology for the purpose of enhancing gas-separation efficacy. Many different types of membranes and membrane processes have been reported in this spirit, including supported IL membranes (SILMs), polymerized ionic liquid (PIL) membranes, polymer/IL gel membranes, as well as membrane contactors (MCs) using ILs as an absorbent.[3–5]

Numerous hybrid membranes that embed an IL into a polymeric matrix have been developed, since they can be readily prepared by mixing the IL with a variety of polymers in suitable solvents, and their gas-transport properties can be adjusted by controlling the concentration of added IL.[6] For instance, neutral polymers such as a poly(ether-*b*-amide) block copolymer (Pebax®), poly(vinylidene fluoride-*co*-hexafluoropropylene) P(VDF-HFP), poly(vinylidene fluoride) (PVDF), and polyimides (PIs) have been successfully used to prepare polymer/IL membranes.[7–11] By judiciously choosing the polymer matrix and IL additive, significant improvements in both gas permeability and selectivity can be achieved.[10,12] A non-negligible drawback, however, is that the low-molecular-weight constituents of ILs gradually leach out of the membrane over time, thereby promoting a corresponding loss of separation performance. To overcome this challenge, independent research efforts have sought to employ polyelectrolytes as the polymeric matrix in polymer/IL membranes, since the intermolecular interactions between the charged polymer chains comprising the polyelectrolyte and the mobile IL mole-

[a]Department of Chemical Engineering, Norwegian University of Science and Technology Trondheim, 7491, Norway. E-mail: deng@nt.ntnu.no; Tel: +47 73594112
[b]Department of Materials Science & Engineering, North Carolina State University, Raleigh, NC 27695, USA
[c]Department of Chemical & Biomolecular Engineering, North Carolina State University, Raleigh, NC 27695, USA
† These authors contributed equally to this work.

cules are stronger than those with uncharged polymers (due to the additional Coulombic attractions between the charged species).[13,14] Furthermore, some polyelectrolytes (e.g., PILS) can form miscible (molecular) solutions with ILs at IL loading levels as high as 60 wt% as a consequence of the inherently strong ionic interactions between the solid and liquid components.[14] Despite the potentially large number of polyelectrolytes available as homo(PIL)s or polymerized ionic liquid block copolymers (PIL-BCPs) available for polymer/IL membranes, such hybrid membranes generally require multiple synthesis steps and tend to be relatively expensive.[15]

Sulfonated ionomers have recently received increasing attention for membrane-based CO_2 capture applications.[16,17] Among this class of polymers, Nafion is a well-established polyelectrolyte commonly used as a polymer electrolyte membrane (PEM) in low-temperature fuel cells and water electrolyzers.[18] It belongs to the family of sulfonated tetrafluoroethylene-based fluoropolymer-copolymers developed in the late 1960s by DuPont. Due to its robust mechanical, thermal and chemical stability and, most importantly, its high proton conductivity, Nafion has remained the subject of tremendous fundamental and technological interest over the past few decades.[18] In this vein, numerous studies have examined the gas permeabilities of H_2 and O_2 in Nafion membranes intended for fuel cell applications.[19] Significantly fewer reports have endeavored to apply Nafion membranes for CO_2 gas separation due to its unacceptably low permeability (≈ 2.0 Barrer) and selectivity (about 8–10 relative to N_2).[20–22]

Mauritz et al.[23] have reported that the hydrophilic sulfonic acid (–SO_3H) moieties can aggregate and form ionic clusters in the neat Nafion matrix. These ionic clusters are interconnected and can form ionic nanoscale channels ranging in size from ca. 1.5 to 5.0 nm.[24,25] Such nanochannels are sensitive to the presence of water in Nafion membranes and gradually swell with increasing water content.[26] For this reason, the gas-transport properties of Nafion have been interrogated under humid conditions and reveal remarkable enhancement (up to 2 orders of magnitude) of the permeability coefficient for various gaseous species.[22] The response of the nanochannels to water is believed to contribute largely to the transport of gases (as well as protons) in Nafion membranes. Nevertheless, gas permeability data reported for Nafion under humid conditions have been previously obtained using extruded membranes. Since this fabrication route produces relatively thick samples (>25 μm), it cannot be implemented in the fabrication of thin composite membranes composed of thin (~1 μm or lower) dense selective layers. Yoo et al.[27] have previously attempted to fabricate hybrid Nafion/IL membranes from IL-imbibed films to improve CO_2/CH_4 separation. However, as the IL could only induce swelling by adsorbing into and diffusing through the existing ionic cluster channels constrained by the rigid Nafion matrix with limited IL sorption, only a small amount of IL (up to 10 wt%) could be introduced into the membrane. Such membranes display a relatively limited effect on gas-transport properties. Sun and Zhou[28] have modeled the spatial distribution of ILs in Nafion and demonstrated that, by

swelling, the IL could not form a continuous phase until the amount of incorporated IL reaches 57%. Membranes generated by solvent casting are therefore preferable, but prior attempts to use solvent-cast Nafion membranes have resulted in reduced gas-separation performance.[29,30]

In the present study, Nafion and the IL 1-butyl-3-methylimidazolium tetrafluoroborate ([Bmim][BF_4]) are selected to prepare hybrid polymer/IL membranes for CO_2 separation. Due to its established high CO_2 affinity and CO_2 solubility selectivity over other gases, [Bmim][BF_4] is ideally suited as the "first promoter" to enhance gas permeability. Membranes containing up to 40 wt% IL have been prepared, and the physical and chemical properties of the resultant membranes have been characterized by various analytical techniques. Single-gas permeation of gases including He, CO_2, N_2, and CH_4 has been systematically studied at different temperatures in the dry state. In addition, because of the nontrivial effect of absorbed water on membrane nanostructure and gas transport,[31] water vapor is employed as the "second promoter" to improve gas permeability. For this reason, the water uptake of Nafion/IL membranes is also investigated at 100% RH, and mixed-gas permeability tests of CO_2/N_2 in Nafion/IL membranes at various RH conditions are used to elucidate the role of water on the transport properties of these hybrid membranes. Despite various attempts to improve the gas permeability of Nafion, however, the synergistic effects of IL and water on Nafion transport properties have not, to the best of the authors' knowledge, been investigated for gas-separation purposes involving CO_2. We propose that an optimum synergy can be achieved between both promoters so that CO_2 permeability can be greatly enhanced, thus ensuring superior separation performance.

2. Experimental

2.1. Materials

Alcohol-based Nafion solutions (5 wt%, D520, total acid capacity of 1.03–1.12 meq g^{-1}, equivalent weight [EW] = 1100 $g_{polymer}$ mol$_{SO_3}^{-1}$) and extruded Nafion sheets (~25 μm thick) were obtained from Ion Power (Munich, Germany), whereas [Bmim][BF_4] (97% purity) was purchased from Sigma-Aldrich (Buchs, Switzerland) and used without further purification. The gases examined in the gas permeation tests included a CO_2/N_2 mixture, CO_2, He, N_2, and CH_4 and were purchased from AGA (Oslo, Norway) and used as-received. The purity of the single gases was 99.999%.

2.2 Membrane preparation

A desired amount of Nafion solution was mixed with a calculated amount of [Bmim][BF_4] in a glass vial and subjected to magnetic stirring for at least 30 min. The solution was then poured into a glass Petri dish and heated to 80 °C for 100–120 min to generate uniform and un-cracked membranes.[32] (Heating was required to ensure the generation of uniformly homogeneous films.) A second glass Petri dish was used to cover the first one to reduce the rate of solvent evaporation. After the

solvent evaporated, the resulting membrane was dried under vacuum at 60 °C for at least 6 h prior to testing. Membrane thicknesses were measured with a Digimatic ID-H thickness gauge (Mituyoto, Aurora, IL) as the average of at least 10 measurements over the entire permeating area. The IL content (ω_{IL}, wt%) in each hybrid membrane was calculated from

$$\omega_{IL} = \frac{w_{IL}}{w_{IL} + w_{Nafion}} \times 100 \qquad (1)$$

where w_{IL} and w_{Nafion} are the weights of [Bmim][BF$_4$] and Nafion, respectively.

2.3 Membrane characterization

The thermal stability of the Nafion/IL membranes was investigated by thermogravimetric analysis (TGA) performed on a TA Q500 instrument. Samples weighing 5–10 mg were placed in sample pans and heated from ambient temperature to 550 °C at a heating rate of 10 °C min^{-1}. To prevent premature degradation, nitrogen was used as an inert sweep gas at a flow rate of 60 mL min^{-1}. Fourier-transform infrared (FTIR) spectroscopy was performed on a Thermo Nicolet Nexus spectrometer with a smart endurance reflection cell. All spectra were recorded in attenuated total reflectance (ATR) mode with a diamond crystal. This chemical analysis was conducted on neat [Bmim][BF$_4$], neat Nafion and Nafion/IL hybrid membranes at various IL concentrations to discern if the two constituents interact chemically and, if so, which functionalities were involved. Spectra were averaged over 16 scans at a wavenumber resolution of 4 cm^{-1}. The nanostructures of neat Nafion and several Nafion/IL membranes were characterized by small-angle X-ray scattering (SAXS) performed on beam-line 12-ID-B in the Advanced Photon Source at Argonne National Laboratory. The sample-to-detector distance and beam spot size were 2 m and 0.5 × 0.025 mm^2, respectively, and samples were exposed to a 14 keV beam (with a wavelength, λ, of 0.087 nm). Data collected on a 2-D Pilatus 2 M detector were azimuthally integrated to yield scattering profiles in which intensity is expressed as a function of scattering vector (q), where $q = (4\pi/\lambda)\sin\theta$ and θ is half the scattering angle.

The water uptake of various membranes was measured by placing the samples in a closed volume saturated with water vapor at ambient temperature and atmospheric pressure, followed by weighing at various times after initial exposure. The sample weight was recorded until a constant value was obtained, ensuring that equilibrium was reached. Values of water uptake (Ω_{H_2O}, expressed in terms of g_{H_2O}/g_S, where g_S refers to the overall mass of the dry sample) were computed from

$$\Omega_{H_2O} = \frac{w_\infty - w_D}{w_D} \times 100 \qquad (2)$$

where w_D and w_∞ correspond to the weights of dry and water-saturated membranes, respectively. The water uptake of the membranes was estimated from the average value of two samples with an error of less than 5%. In the present study, single-gas permeability values were measured using a constant-volume variable-pressure method,[33] similar to that

reported elsewhere.[34] After thorough evacuation of the membrane to remove all previously dissolved species, the membrane was exposed to the feed gas, and the pressure in the fixed permeate volume was continuously monitored. A leak test was performed before starting each test. Measurements were conducted with He, CH$_4$, N$_2$, and CO$_2$. Helium permeation was measured instead of hydrogen for safety reasons.[35] Single-gas permeability (P_s) was determined from the rate of downstream-pressure increase $\left(\frac{dp_d}{dt}\right)$ achieved when permeation reached steady state according to

$$P_s = \left[\left(\frac{dp_d}{dt}\right)_{t\to\infty} - \left(\frac{dp_d}{dt}\right)_{leak} \right] \cdot \frac{V_d l}{RTA(p_u - p_d)} \qquad (3)$$

where V_d is the downstream volume, l is the membrane thickness, A refers to the effective permeation area, T denotes absolute temperature, R is the universal gas constant, and p_u and p_d represent the upstream and downstream pressures, respectively. For each membrane, two samples were tested with a relative error less than 10%, and the final result is reported as the average of the two measurements. The corresponding ideal selectivity between two gases A and B ($\alpha_{A/B}{}^i$) is given by

$$\alpha_{A/B}{}^i = \frac{P_{s,A}}{P_{s,B}} \qquad (4)$$

where $P_{s,A}$ and $P_{s,B}$ correspond to the single-gas permeabilities of species A and B, respectively. Gas-separation performance was furthermore measured with the mixed-gas setup schematically depicted in Fig. 1. The membrane was placed inside a sample holder with a permeating area of 19.6 cm^2. Before each permeation test, membranes were conditioned by blowing humid feed/sweep gas to the desired RH conditions. A 10/90 v/v CO$_2$/N$_2$ gas mixture constituted the feed gas, whereas pure CH$_4$ was the sweep gas. The humidity of both feed and sweep streams was accurately adjusted by using mass flow controllers (El-Flow series, Bronkhorst). A back-pressure regulator (El-Press series, Bronkhorst) controlled the feed-side pressure. Pressures were monitored (Wika, S-10) and held constant at 2.0 bar on the feed side and up to 1.05 bar on the sweep side for all the experiments. The compositions of retentate and permeate streams exiting the membrane module were monitored by a calibrated gas chromatograph (490 Micro GC, Agilent) over the duration of the test. Each test continued for at least 3 h to ensure steady state.

The permeability coefficient (P_i) of the ith penetrant species was measured by

$$P_{m,i} = \frac{N_{perm}(1 - y_{H_2O})y_i l}{A(p_{i,feed}, p_{i,ret} - p_{i,perm})} \qquad (5)$$

where N_{perm} is the total permeate flow measured with a bubble flow meter, y_{H_2O} is the molar fraction of water in the permeate flow (calculated according to the RH value and the vapor pressure at the given temperature), y_i is the molar fraction of the species of interest in the permeate, and $p_{i,feed}$, $p_{i,ret}$ and $p_{i,perm}$ identify the partial pressures of the ith species in the
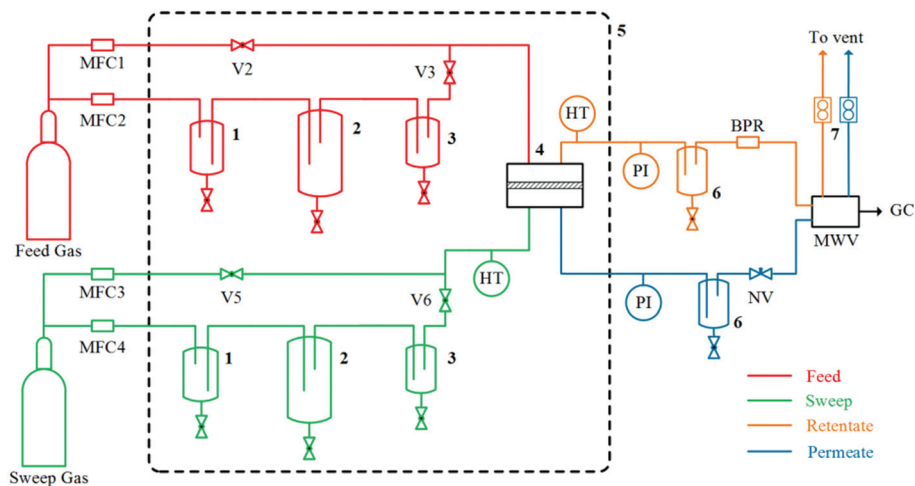
Fig. 1 Mixed-gas permeation setup (1: MFC-safety trap; 2: humidifier; 3: droplets trap; 4: membrane module; 5: heated cabinet; 6: water knockout; 7: bubble flow meters; MFC: mass flow controller; NV: needle valve; BPR: back-pressure regulator; PI: pressure indicator; HT: humidity and temperature sensor; MWV: multi-way valve; GC: gas chromatograph).

feed, retentate and permeate, respectively. As in eqn (3), A corresponds to the permeating area in eqn (5). The separation factor $\left(\alpha_{i/j} = \dfrac{y_i/x_i}{y_j/x_j} \right)$ was applied for mixed-gas permeation tests. It is worth mentioning that, while the ideal selectivity $\left(\alpha_{A/B}{}^i = \dfrac{P_{s,A}}{P_{s,B}} \right)$ was also determined here, variation between ideal selectivity and separation factor was less than 5%, in which case only the separation factor is reported. Because of measurement differences in the permeation setups, specimens for single-gas permeation tests ranged in thickness from 50 to 75 μm, whereas film thicknesses were reduced to 15–25 μm for mixed-gas permeation tests.

3.   Results and discussion

3.1   Characterization of neat Nafion membranes

Neat Nafion membranes can be fabricated *via* solvent casting or extrusion. In the present work, the first procedure is followed to prepare pure Nafion and hybrid Nafion/IL membranes. To ensure a suitable benchmark, we begin with an assessment of pure Nafion membranes by comparing cast membranes with commercially available extruded film in terms of transport properties. Doing so also permits direct comparison with previously reported data, since the gas transport properties under humid conditions have only been reported for extruded Nafion.[22] Results obtained from mixed-gas tests are displayed in Fig. 2. As expected, CO_2 permeability in the Nafion membrane increases with increasing RH to a significant extent (>100-fold enhancement). In addition, our results obtained for extruded Nafion are in favorable agreement with literature values.[22] Differences in feed conditions (*e.g.*, the CO_2 partial pressure on the feed side of the membrane is 0.2 bar in our experiments but 2.0 bar in ref. 22) have a negligible effect on transport properties, as no swelling or relaxation phenomena are expected in this CO_2 pressure range. Similar conclusions can be also drawn for the CO_2/N_2 selectivity, as the results obtained from our experiments are in the same range as the ones reported elsewhere.[22]
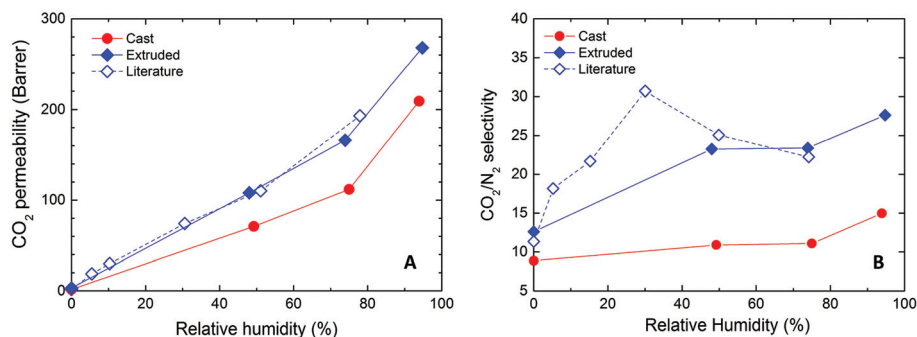

Fig. 2   (A) CO_2 permeability and (B) CO_2/N_2 selectivity as functions of RH for Nafion membranes obtained by solvent casting and extrusion. The literature data are obtained from ref. 22.

As can be seen from Fig. 2, the membrane fabrication procedure clearly influences the apparent transport properties, since solvent-cast Nafion possesses a noticeably lower (25–35%) CO_2 permeability compared to that of the extruded film over the entire RH range. Similar reductions (by about 50%) are also obtained for the separation factor. We propose that the two fabrication methods produce different nanostructures within the Nafion membranes, which result in different molecular transport properties. While exploration of the mechanism underpinning this observation warrants further study, it is beyond the scope of the current work. Moreover, insufficient information regarding the extrusion conditions for commercial Nafion severely limits the feasibility of further study. Therefore, the present study will focus exclusively on solvent-cast Nafion membranes and all further reference to Nafion will hereafter pertain to these membranes.

3.2 Ionic liquid selection

According to the two-pronged strategy adopted in the present work, ILs serve as the "first promoter" to enhance the permeability of gases in Nafion membranes. The initial selection of ILs in the fabrication of these hybrid membranes relies on the chemisorption of ILs with specific CO_2 reactivity, as they are expected to provide higher CO_2 selectivity and CO_2 sorptive capacity. Specifically, 1-ethyl-3-methylimidazolium bis(trifluoromethanesulfonyl) imide ($[Emim][Zn][(Tf_2N)_3]$)[36] and 1-butyl-3-methylimidazolium bis(trifluoromethanesulfonyl) imide ($[Bmim][Zn][(Tf_2N)_3]$) containing Zn^{2+}, as well as trihexyl(tetradecyl)phosphonium prolinate ($[Pro][P_{66614}]$) and glycinate ($[Gly][P_{66614}]$),[37] have been synthesized and mixed with the starting Nafion solution. The chemical structures of these ILs considered in the present study are included in Fig. 3. Unfortunately, we have had no success in fabricating an acceptable membrane with most of these ILs, likely due to the strong interactions between the sulfonic acid groups present on Nafion and the basic moieties in the ILs. Such interactions induce visible macrophase separation, thus impeding the formation of a homogeneous membrane. As a consequence of this explanation, a physisorption-based IL is believed to be more likely to succeed because it possesses no reactive groups that can interact with the polymer during membrane preparation. In this vein and among the various IL options available, $[Bmim][BF_4]$ is found to yield satisfactory membranes and is remarkably suitable for the present investigation on the basis of its high CO_2 solubility, CO_2 diffusivity and CO_2/N_2 selectivity.[38] Another benefit of this IL is that addition of a small concentration of water to $[Bmim][BF_4]$ has been reported[39] to promote a significant drop in viscosity (∼50%), which might serve to enhance the diffusion coefficient of small molecules. For the above reasons, visually homogeneous, self-standing Nafion/$[Bmim][BF_4]$ membranes are only considered further in this study.

3.3 Physical and chemical characterization

3.3.1 Thermal properties. Results from TGA of the IL, Nafion and hybrid Nafion/IL membranes are presented in Fig. 4. In the case of pure $[Bmim][BF_4]$, a decomposition tem-
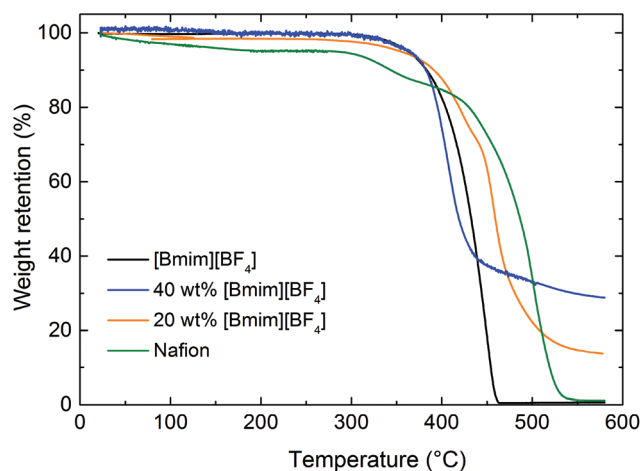

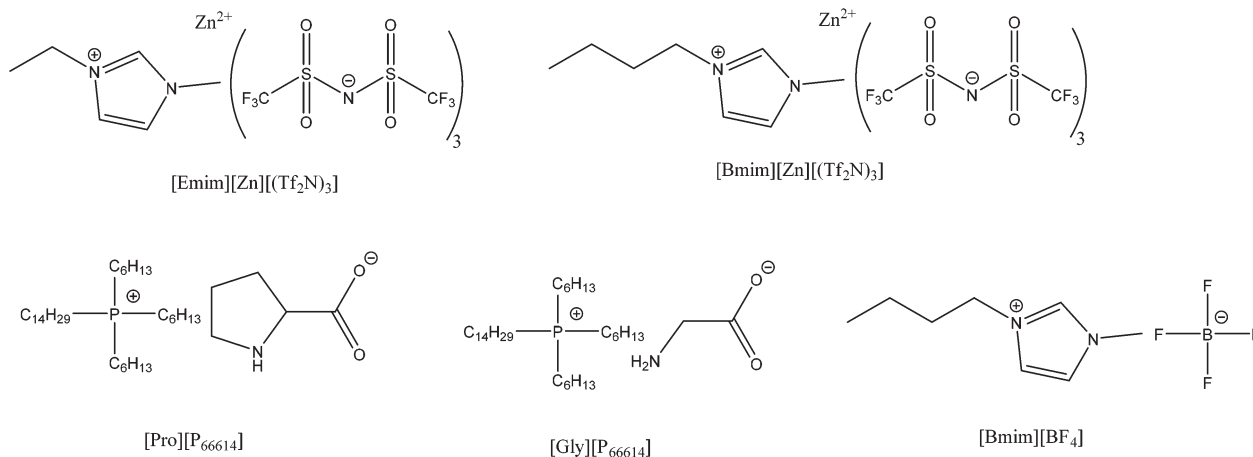Fig. 4 TGA results from Nafion, IL and Nafion/IL membranes (labeled).

Fig. 3 Chemical structures of the ILs considered in the present study.

perature of around 450 °C is evident, which is in favorable agreement with previous results.[40] According to several independent sources,[41–43] production of a completely anhydrous Nafion membrane is not possible without destroying the sample. Even after long periods of vacuum-drying, residual water (≈ 3%) remains in the membrane, and this corresponds to about 1.5 H_2O molecules/sulfonic acid group.[42] In this study, mass loss (about 6% of the initial weight) was observed for pure Nafion at ≈100 °C, suggesting that water remains in the membrane even after drying under vacuum for more than 6 h. A second, more pronounced mass loss is apparent from 290 to 420 °C, which is likely associated with desulfonation,[43] while a precipitous drop over 400–530 °C is attributed to side-chain and/or backbone decomposition,[42] which has been reported above 500 °C.[44]

For both Nafion/IL composite membranes investigated by TGA, specimen mass losses are nearly negligible at temperatures below 350 °C. This result suggests that interactions occur between the IL, sulfonic acid groups and H_2O molecules, in which case any residual water in the Nafion matrix becomes undetectable, and the thermal stability of the hybrid membranes is improved. As expected for many organic compounds, the mass loss for pure [Bmim][BF$_4$] and Nafion is nearly 100% over 600 °C, implying that most of the materials decompose to gaseous products at these elevated temperatures. In the case of the Nafion/IL hybrid membranes, however, considerable residual mass remains detectable at the same temperature and appears to be directly related to the IL content in the membrane. One explanation for this unexpected outcome regarding the Nafion/IL membranes relates to the formation of new ion pairs between the IL and sulfonic acid groups in Nafion matrix. These ion pairs could stabilize C–S bonds and gradually enhance thermal stability,[45] thereby providing an attractive materials design paradigm for high-temperature applications. Another possible explanation for our observation is that the side chains in Nafion might chemically react with [Bmim][BF$_4$] at high temperatures and form a more stable chemical compound that pyrolyzes to carbon instead of vaporizing at temperatures in the vicinity of 600 °C.

3.3.2 FTIR analysis. In this study, FTIR spectroscopy has been employed to discern the existence of possible ion–polymer interactions or reactions, and identify the conformational changes in Nafion due to the physical incorporation of IL. Representative FTIR spectra acquired from 800 to 1800 cm^{-1} for Nafion, IL and Nafion/IL membranes with different concentrations of [Bmim][BF$_4$] are displayed in Fig. 5. Only this region is displayed since the primary peak vibrations corresponding to both Nafion and the IL reside in this so-called fingerprint region. The spectrum acquired from [Bmim][BF$_4$] is characterized by a very strong multimodal peak associated with B–F stretching in [BF$_4$]$^-$ between about 950 and 1150 cm^{-1}, whereas the peaks positioned between 1550–1600 cm^{-1} and 1150–1200 cm^{-1} are a consequence of in-plane C–C and C–N vibrations, respectively, of the imidazole ring.[46–48] The spectrum collected from Nafion displays two strong vibrations related to symmetric C–F stretching
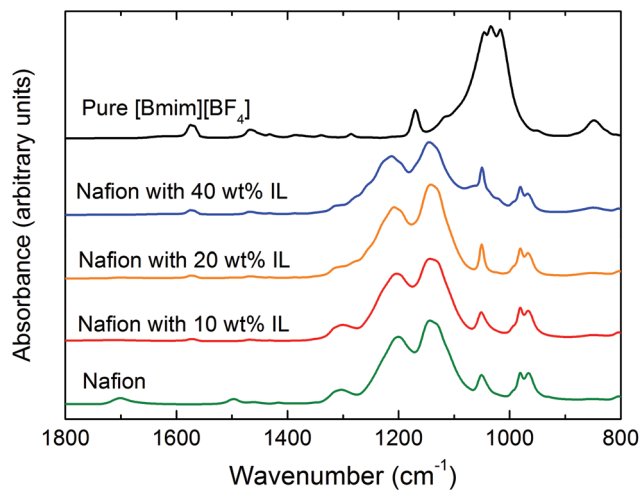

Fig. 5 FTIR spectra of Nafion, IL and Nafion/IL membranes (labeled).

(~1160 cm^{-1}) and asymmetric C–F stretching (~1200 cm^{-1}).[49] The remaining peaks, related to C–F, C–O–C and S–O bonds, are consistent with previous findings.[50–53] Broad peaks observed at ~1710 cm^{-1} and in the region between 3000 and 3600 cm^{-1} (data not shown) reflect the bending[49] and stretching[50] vibrations of H_2O and H_3O^+, respectively. Interestingly, comparison of the pure Nafion spectrum with those obtained from the Nafion/IL hybrid membranes reveals that incorporation of IL within the Nafion matrix promotes a significant reduction in the amount of water present, even at the lowest IL loading level examined. This change strongly suggests the existence of direct interaction between the added IL and the sulfonic acid groups responsible for displacing water molecules typically bound to the sulfonic acid moieties. Furthermore, the accompanying decrease in the small peak positioned at ~1300 cm^{-1}, which is attributed to SO$_3^-$ stretching from water-induced dissociation of SO$_3$H groups, provides an independent indication of reduced water content in the hybrid membranes due to interaction between the sulfonic acid groups and the IL. Another IL-induced spectral change involves the peak present in the Nafion spectrum at ~1050 cm^{-1}. This peak becomes sharper and broader as the IL level in the matrix is increased, ultimately evolving into the large peak characteristic of pure [Bmim][BF$_4$]. Since no additional peaks indicative of new chemical bonds are evident in these spectra, we conclude that no chemical reaction occurs between Nafion and [Bmim][BF$_4$].

3.3.3 SAXS analysis. The SAXS profile acquired from Nafion in Fig. 6 appears qualitatively similar to that previously reported by Haubold *et al.*[54] Of particular interest in their data is a relatively broad peak that appears in the vicinity of $q = 1.5$ nm^{-1}. This is referred to as the "ionic peak" and corresponds to an interplanar distance (d) of about 4.2 nm (from Bragg's law, $d = 2\pi/q$). A similarly broad feature appears in Fig. 6, but at $q = 2.2$ nm^{-1} ($d = 2.9$ nm). This moderate inconsistency is attributed to differences in material composition and/or processing and supports our earlier contention based
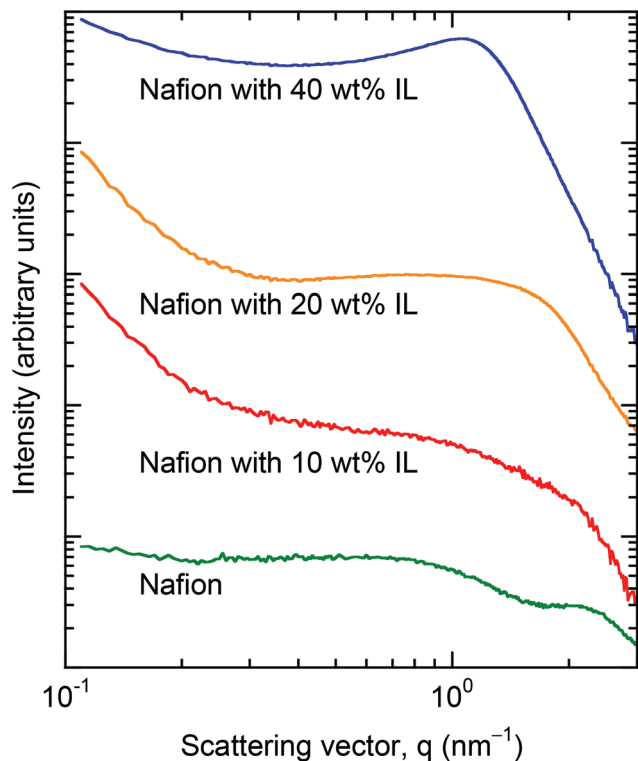
Fig. 6 SAXS profiles of Nafion, IL and Nafion/IL membranes (labeled).

on the results presented in Fig. 2 that variations in material properties and/or processing can impact the resulting nanostructure of Nafion. Addition of 10 wt% IL promotes significant scattering at low q (large dimensions) at the expense of concealing the ionic peak, suggesting that the IL might not distribute uniformly at low loading levels. As the concentration of IL is increased, however, scattering at higher q (not far from the ionic peak) progressively increases, ultimately generating a new scattering peak near q = 1.1 nm^{-1} (d = 5.7 nm). This is consistent with the IL distributing thoroughly throughout the Nafion matrix.

Haubold *et al.*[54] propose a sandwich model to analyze their SAXS results. The components of this model include a highly incompatible fluorocarbon phase, an interphase wherein the sulfonic acid groups reside and a solution regime in the presence of a polar solvent. In their study, they examine the nanostructure of Nafion in the presence of water/methanol cosolvents. Recent cryo-transmission electron microtomography images[55] indicate, however, that a sandwich representation might constitute an oversimplification of the Nafion nanostructure especially at low q. Even without application of the scattering model developed by Haubold *et al.*,[54] their SAXS results of Nafion in the presence of water and pure methanol are nonetheless useful for comparison with our data collected from Nafion/IL membranes. In the cases of water and methanol, scattering is observed to increase slightly beyond that of neat Nafion at low q, but the ionic peak remains clearly unobstructed. This trend is not evident in Fig. 6, suggesting that

the addition of IL induces a composition-dependent rearrangement of the Nafion nanostructure rather than simply inducing swelling. Although detailed morphological analysis of Nafion/IL membranes by electron microscopy or microtomography would likely elucidate IL-induced morphological alteration, such characterization is beyond the scope of the present work.

3.3.4   Water uptake. The transport properties of Nafion are reported[56] to be significantly affected by the presence of water, with an overall permeability enhancement of about two orders of magnitude at the highest humidity. Moreover, the quantity of absorbed water within the Nafion matrix plays a significant role in gas transport, since the Nafion nanochannels filled upon water absorption favor transport of water-soluble gases (*e.g.*, CO_2) over penetrants with lower water solubility (*e.g.*, N_2 and CH_4). The water uptake of Nafion and Nafion/IL membranes at various IL concentrations has been investigated, and representative results are displayed in Fig. 7. The neat Nafion membranes exhibit a water uptake level of 22%. Increasing the IL content in the membrane, however, yields an unexpected trend: the water uptake in Nafion/IL membranes composed of 10 and 20 wt% [Bmim][BF$_4$] is lower than that observed in the neat Nafion membrane, whereas a further increase in IL content to 40 wt% generates a much higher water uptake (42%) that is nearly double that of neat Nafion.

It is well accepted that the highly hydrophilic sulfonic acid anions in Nafion can form dispersed ionic clusters with diameters of ≈1.5 nm throughout the Nafion matrix.[57,58] These ionic clusters play an important role in localized hydration and, thus, water uptake. When the [Bmim][BF$_4$] is added to the polymeric matrix at low concentrations, however, new ion pairs are likely to form due to the strong ion-ion interaction between sulfonic acid and the IL and this could promote a nontrivial change in both the population and composition of the ionic clusters. Such variation is expected to have a negative impact on water uptake since the ions become bound together to yield a neutral charge. As the concentration of IL is
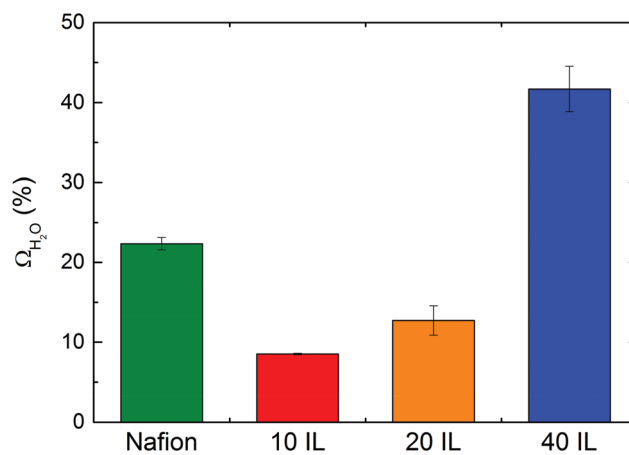

Fig. 7 Water uptake of Nafion and Nafion/IL membranes at atmospheric temperature and pressure and 100% RH (10 IL = 10 wt% [Bmim][BF$_4$], 20 IL = 20 wt% [Bmim][BF$_4$], 40 IL = 40 wt% [Bmim][BF$_4$]).

increased in the Nafion/IL membranes, the distribution of IL is more uniform throughout the material (as evidenced by SAXS in Fig. 6), resulting in unbound (free) IL that, due to the hydrophilic nature of [Bmim][BF$_4$], ensures enhanced water uptake in Nafion/IL membranes at high IL concentrations.

3.4 Single- and mixed-gas permeation studies

3.4.1 Effect of composition on gas permeation. Single-gas permeation tests of the Nafion/IL membranes have been performed using the constant-volume variable-pressure method. Membranes with different IL concentrations have been subjected to a feed pressure of 2.0 bar for CO$_2$, He and N$_2$. As reported elsewhere,[20,57] the permeability of gases in dry Nafion is low compared to several common polymer membranes [*e.g.*, polyimide, poly(ethylene oxide) and Pebax®]. Helium possesses a higher permeability relative to other gases such as N$_2$ and CH$_4$ due to its smaller kinetic diameter. In this study, the permeabilities of He and CO$_2$ in Nafion at ambient temperature are 35 and 1.6 Barrer, respectively, which agrees favorably with previous results.[57] Addition of [Bmim][BF$_4$] significantly enhances the gas transport properties of the hybrid membrane, as confirmed by the results provided in Fig. 8A. For instance, the permeability of CO$_2$ in the Nafion/IL membrane with 40 wt% [Bmim][BF$_4$] is 75.4 Barrer, which is about 50× that of the neat Nafion membrane (*cf.* Fig. 8B). The permeability of N$_2$ also increases due to incorporation of the IL, but the extent of the increase is smaller compared to that of CO$_2$. More specifically, the N$_2$ permeability is enhanced by 10× for the hybrid Nafion/IL membrane with the highest IL content relative to the pristine Nafion membrane. Therefore, these hybrid membranes exhibit significant improvement in terms of the ideal CO$_2$/N$_2$ selectivity, as evidenced in Fig. 9. In particular, a selectivity of 35 is realized for the hybrid membrane with 40 wt% [Bmim][BF$_4$], corresponding to 4× enhancement compared to the neat Nafion membrane, which exhibits a CO$_2$/N$_2$ selectivity of 8.9. These results clearly establish that
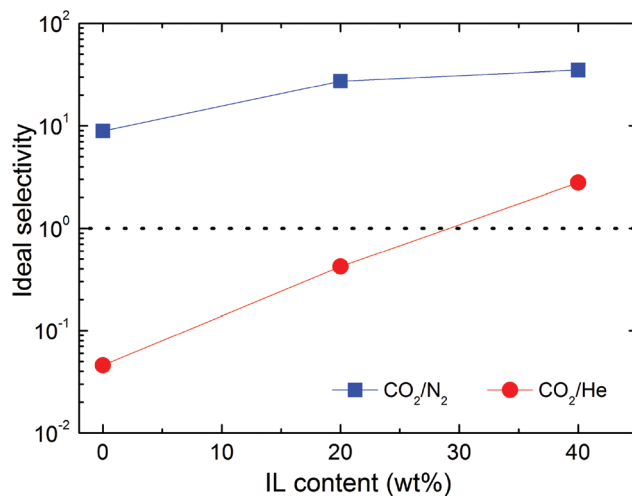

Fig. 9 Ideal selectivity of two gas pairs (color-coded) in Nafion/IL membranes containing different IL concentrations at ambient temperature and 2.0 bar.

the addition of IL to Nafion serves to improve gas transport (as the "first promoter"), enriching the separation performance of Nafion-based membranes both in terms of membrane throughput and separation efficiency. Furthermore, compared to the case wherein IL is imbibed into existing Nafion films,[27] blending Nafion and IL during solution casting appears to be a more successful route by which to distribute IL throughout the Nafion matrix and thus improve the overall CO$_2$ separation performance of the hybrid membrane.

Interestingly, addition of IL to Nafion has limited impact on He gas transport. In fact, He permeability decreases in the hybrid membranes, regardless of the amount of IL contained in the matrix. For this reason, the neat Nafion membrane can be considered He-selective (CO$_2$/He selectivity of 0.046), while the hybrid membrane with 40 wt% [Bmim][BF$_4$] becomes CO$_2$-selective, as indicated in Fig. 9, with a selectivity of 2.7. A poss-
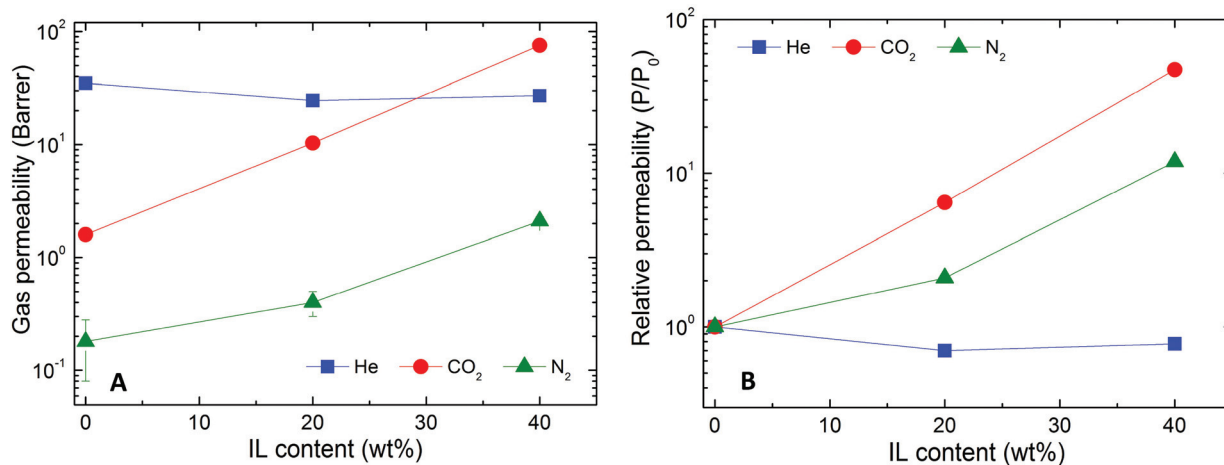

Fig. 8 Permeability (A) and relative permeability (B) of several gases (color-coded) in Nafion/IL membranes containing different IL concentrations at ambient temperature and 2.0 bar.

ible explanation for this observed phenomenon relates to the influence of gas solubility, which is markedly larger in the hybrid membranes compared to neat Nafion. In this scenario, the permeability of gases in the hybrid membranes is anticipated to increase considerably with increasing condensability so that highly condensable gases (*e.g.*, CO_2) are more profoundly affected than less condensable ones (*e.g.*, N_2 and He).

3.4.2 Effect of temperature on gas permeability. The effect of temperature on gas permeability in polymer membranes is dictated by the nature of the polymer (*i.e.*, glassy or rubbery) under specific test conditions. Over a temperature range that does not introduce significant thermal transitions for a given polymer, the temperature dependence of gas permeability (P) can often be described by an Arrhenius equation[59] of the form reported in eqn (6), where P_0 is a pre-exponential factor and E_P is the apparent activation energy for permeation:

$$P = P_0 \exp\left(-\frac{E_P}{RT}\right) \tag{6}$$

The dependence of gas permeability on temperature for the Nafion/IL membrane containing 40 wt% [Bmim][BF$_4$] is evident in Fig. 10. As expected, these results confirm that all the gas permeabilities increase with increasing temperature (*cf.* Table 1), suggesting that diffusion dominates permeation. Since permeability is an example of a thermally-activated mole-
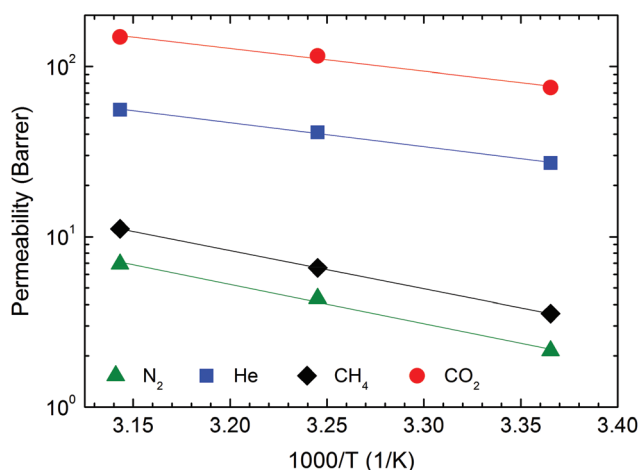
Table 2 Activation energy of permeation for different gases in 40 wt% [Bmim][BF$_4$] Nafion/IL hybrid membranes

	CO_2	N_2	CH_4	He
E_P (kJ mol^{-1})	25.6	44.0	42.9	27.0

cular process, regression of the linear relationship between log (P) and T^{-1} according to the Arrhenius relationship can yield E_P. In this study, the correlation coefficient (R^2) is always greater than 0.99 over the temperature range considered (25–45 °C) for all four tested gases. Extracted values of E_P are listed in Table 2. Similar to many other polymeric membranes (*e.g.*, polyether, Pebax® and polyimide), CO_2 exhibits the lowest activation energy in Nafion/IL membranes compared to other gases of comparable size, such as N_2 and CH_4.[60,61]

Fig. 11 displays the effect of temperature on the ideal gas selectivities α_{CO_2/N_2}, α_{CO_2/CH_4} and $\alpha_{CO_2/He}$ at 2.0 bar. As anticipated from the larger values of E_P for N_2 and CH_4 relative to that of CO_2, both α_{CO_2/N_2} and α_{CO_2/CH_4} decrease significantly when temperature is increased from 25 to 45 °C. This observation reflects a corresponding reduction in solubility selectivity due to the sharp temperature-driven decrease of CO_2 solubility in [Bmim][BF$_4$]. Concurrently, the diffusivity of gases possessing a larger kinetic diameter (*e.g.*, N_2 and CH_4) is more noticeably influenced by the increase in operating temperature relative to smaller penetrants (*e.g.*, CO_2), which also negatively affects membrane selectivity.[62]

3.4.3 Effect of humidity on gas permeability. The permeation properties of Nafion/IL hybrid membranes have also been studied by using a CO_2/N_2 gas mixture as the feed at various RH levels to ascertain the effect of the water vapor on molecular transport. The results of this test are presented in Fig. 12A and clearly demonstrate that water vapor has a positive effect on CO_2 permeability in both neat Nafion and
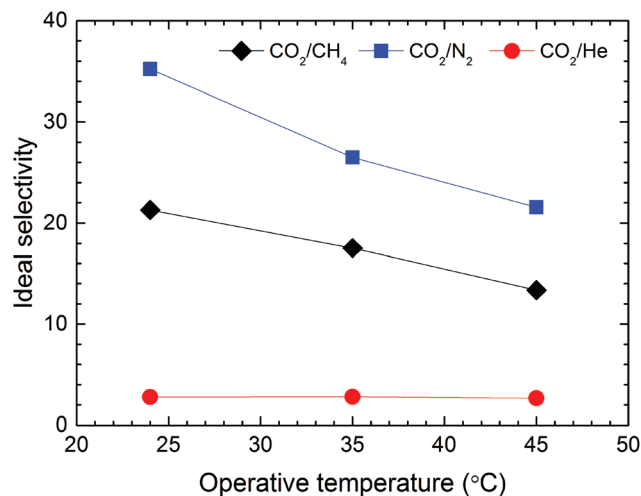

Fig. 10 Permeability of several gases (color-coded) as a function of temperature in the Nafion/IL membrane with 40 wt% [Bmim][BF$_4$] at 2.0 bar.

Table 1 Temperature dependence of single-gas permeability in 40 wt% [Bmim][BF$_4$] Nafion/IL hybrid membranes

	Permeability (Barrer)		
	25 °C	35 °C	45 °C
CO_2	75.4	115.1	148.9
He	27.1	41.0	55.8
N_2	2.1	4.3	6.9
CH_4	3.5	6.6	11.2

Fig. 11 Ideal selectivity of several gas pairs (color-coded) at different temperatures in the Nafion/IL membrane with 40 wt% [Bmim][BF$_4$] at 2.0 bar.
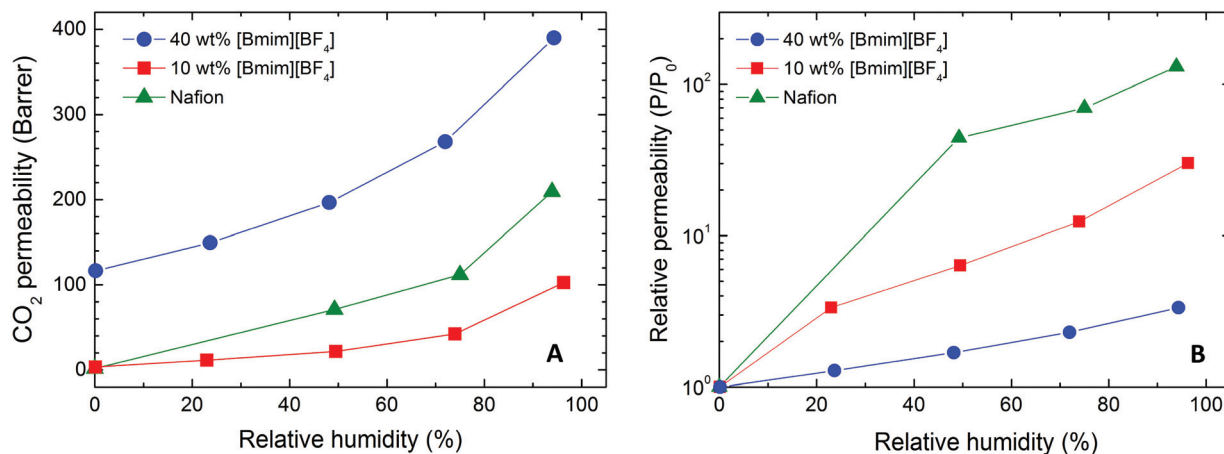
Fig. 12 CO_2 permeability (A) and relative CO_2 permeability (B) of Nafion/IL membranes varying in composition (color-coded) as a function of RH at ambient temperature and 2.0 bar.

Nafion/IL hybrid membranes, since all the measured permeabilities increase with increasing feed gas RH. As seen in this figure, CO_2 permeability in Nafion is improved by two orders of magnitude at the maximum humidity, as the value is increased from 1.6 Barrer in the dry state to 209 Barrer near 100% RH. The presence of water vapor enhances CO_2 permeability in the Nafion/IL membranes as well. At 10 wt% [Bmim][BF$_4$], CO_2 permeability increases from 3.4 to 103 Barrer from the dry state to ~100% RH, while the CO_2 permeability increases from 116 to 390 Barrer over the same humidity range in the Nafion/IL with 40 wt% [Bmim][BF$_4$]. Therefore, we conclude that water vapor significantly improves the CO_2 separation performance of Nafion membranes with and without IL, in which case it can be considered as the "second promoter" for Nafion/IL hybrid membranes. In the case of the Nafion/IL membrane with 40 wt% [Bmim][BF$_4$], performance under fully dry conditions has been measured after the full series of humidified-gas permeation tests, yielding a CO_2 permeability (108 Barrer) in favorable agreement with the value initially obtained. Furthermore, recovery of the initial dry transport properties also suggests that the effect of water vapor is fully reversible, thereby exhibiting good membrane stability over at least ~72 h operation (since the duration of each permeation test is ~12 h).

According to Sarti and co-workers,[22] water-induced enhancement of gas transport in neat Nafion can be traced to different nanoscale morphologies of the membrane. Under dry conditions the ionic clusters formed by sulfonic acid moieties behave as impermeable obstacles for gas diffusion. Upon hydration, nanoscale water channels form and serve as preferential diffusive pathways for the permeation of gas molecules. The solubility of gas penetrants in water therefore plays an important role in determining the effect of water on the permeability coefficient for a specific penetrant. In the case of Nafion/IL hybrid membranes, interactions between the IL moieties and the sulfonic acid groups of Nafion occur in similar fashion as water, as evidenced by the water uptake

results in Fig. 7. At sufficiently high concentrations, the IL molecules are expected to form interconnected nanochannels that function as diffusive pathways for gas transport. Similarly, gas solubility in ILs likewise governs membrane selectivity.

On the basis of the results obtained for the CO_2 permeability at different RH values, the dependence of the relative CO_2 permeability on RH is shown in Fig. 12B. While water vapor appears very effective at promoting CO_2 permeability in neat Nafion (with a 130× increase), an increase in IL content in hybrid Nafion/IL membranes is accompanied by a less pronounced positive effect: 30× and 3× for hybrid membranes containing 10 and 40 wt% [Bmim][BF$_4$], respectively. As alluded to earlier, this phenomenon implies that water vapor can effectively increase the size of the ionic clusters in the polymeric matrix, thus greatly improving CO_2 permeability in neat Nafion membranes. In the Nafion/IL membranes, however, IL molecules interfere with the ionic clusters composed of sulfonic acid groups, according to the FTIR results provided in Fig. 5, and reduce their ionic strength, which, in turn, enhances CO_2 diffusivity through the hybrid membrane matrix. Because of this IL-induced interaction, the effect of water is partially replaced, thereby diminishing the relative influence of water vapor on CO_2 permeability observed in Fig. 12B. Furthermore, under humid conditions, the IL itself is affected by the presence of water, which is expected to promote reductions in both CO_2 solubility and viscosity and a corresponding increase in the diffusion of gaseous penetrants. Although no direct evidence is presently available for [Bmim][BF$_4$], independent studies of similar ILs verify that the first effect is somewhat limited (<15% drop in CO_2 absorptive capacity[63]), whereas the change in viscosity (a 45–75% decrease at ambient temperature[64]) is expected to enhance the diffusion coefficient to a larger extent.[65] Therefore, the enhanced CO_2 permeability due to humidity in the Nafion/IL hybrid membranes visible in Fig. 12A at 40 wt% [Bmim][BF$_4$] is attributed, at least in part, to higher CO_2 diffusivity within the IL.
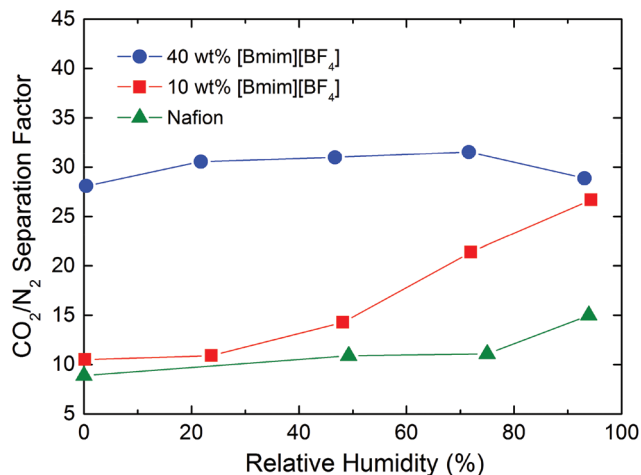
Fig. 13 CO_2/N_2 selectivity in Nafion/IL membranes containing different IL concentrations (color-coded) obtained from mixed-gas permeation tests as a function of RH at ambient temperature and 2.0 bar.

The ideal CO_2/N_2 selectivity (separation factor) of Nafion/IL membranes prepared at various IL concentrations and measured at different RH conditions is displayed in Fig. 13. As discussed in regard to Fig. 8, the CO_2/N_2 selectivity of these hybrid membranes increases with increasing IL content under dry gas feed conditions. The mixed-gas selectivity of the hybrid membrane appears slightly lower compared to the one discerned from single-gas permeation tests, most likely due to the lower partial pressure of CO_2 in the feed gas. Interestingly, an increase in RH in the gas feed manifests a different effect on the CO_2/N_2 selectivity of the hybrid membranes. In the Nafion/IL membrane with 40 wt% [Bmim][BF$_4$], the separation factor (~30) is close to the CO_2/N_2 separation factor obtained from [Bmim][BF$_4$]-based SILMs,[66] indicating that the IL dominates the separation mechanism in the membrane. For neat Nafion and the Nafion/IL membrane with 10 wt% [Bmim][BF$_4$], the CO_2/N_2 selectivity is much lower under dry conditions and increases systematically with increasing RH. On the basis of these observations, we believe that, in the dry state or low RH levels, gas selectivity is determined by the Nafion matrix, while at higher RH values, selectivity is determined primarily by water absorbed in the ionic clusters.[22]

By analyzing the membrane composition at different IL loading levels under the dry and humidified conditions reported in Table 3, we can identify the different contributions of the IL and water on membrane transport properties. Addition of IL only to Nafion promotes a limited interaction with the sulfonic groups present on the polymer chain (up to 3.2 mol$_{IL}$/mol$_{SO_3}$), thereby confirming a positive effect on both CO_2 permeability and selectivity of the membrane. Stronger influence on CO_2 permeability is, however, observed in the presence of H$_2$O, due presumably to the larger population of H$_2$O molecules able to interact with the ionic moieties (up to 41.7 mol$_{H_2O}$/mol$_{SO_3}$). On one hand, if we now consider a comparable concentration (~20 wt%) of IL and H$_2$O in the polymer matrix (*i.e.*, Nafion + 20 wt% [Bmim][BF$_4$] under dry conditions and cast Nafion under fully humidified conditions), H$_2$O appears to be much more effective at enhancing CO_2 permeability (209 *versus* 10 Barrer). On the other hand, the presence of the IL ensures a higher selectivity (27 *versus* 14). Thus, when both IL and water are present in the Nafion matrix, the CO_2 permeability is significantly less sensitive to water content, whereas membrane selectivity increases with increasing IL content, which together illustrate the synergetic effect of IL and H$_2$O in enhancing the overall transport properties of Nafion.

The separation performance of Nafion/IL membranes developed in this study is compared in Table 4 with other perfluorosulfonated membranes and polymer/IL membranes reported in the literature. Moreover, results obtained here are compared with other separation membranes in the Robeson plot[71] provided in Fig. 14. In this figure, neat Nafion membranes exhibit relatively poor gas-transport properties in the dry state, as evidenced by CO_2 permeabilities of ~2 Barrer and CO_2/N_2 selectivities of 8–10. Addition of the "first promoter" ([Bmim][BF$_4$]) significantly improves the transport properties. Simultaneous enhancement of CO_2 permeability and CO_2/N_2 selectivity in the membrane with 40 wt% [Bmim][BF$_4$] brings the separation performance closer to the Robeson upper bound.[71,72] When the "second promoter" (water vapor) is added to the system, both the CO_2 permeability and CO_2/N_2 selectivity improve significantly for the Nafion/IL hybrid membrane with 10 wt% [Bmim][BF$_4$]. In the hybrid membrane with 40 wt% [Bmim][BF$_4$], the CO_2 permeability displays a monotonic increase with increasing RH, while the separation factor remains relatively constant, which allows the separation performance to approach the upper bound. The separation attributes of the membrane containing 40 wt% [Bmim][BF$_4$] are also higher than those of the extruded membranes, thereby confirming that post-combustion CO_2 capture membranes can

Table 3 Membrane composition and separation performance for different [Bmim][BF$_4$] and H$_2$O content in the Nafion matrix

Nafion (wt%)	[Bmim][BF$_4$] (wt%)	H$_2$O (wt%)	[Bmim][BF$_4$] (mol/mol$_{SO_3}$)	H$_2$O (mol/mol$_{SO_3}$)	P_{CO_2} (Barrer)	α_{CO_2/N_2}
1.00	0.00	0.00	0.0	0.0	1.6	9
0.90	0.10	0.00	0.5	0.0	3.4	11
0.80	0.20	0.00	1.2	0.0	10	27
0.60	0.40	0.00	3.2	0.0	116	28
0.81	0.00	0.19	0.0	14.0	209	14
0.83	0.09	0.07	0.5	5.4	102	26
0.43	0.28	0.29	3.2	41.7	329	28

Table 4 Separation performance of selected perfluorosulfonated membranes and polymer/IL membranes

Membrane	P_{CO_2} (Barrer)	α_{CO_2/N_2}	Ref.
Nafion 111 (dry state)	2.3	—	67[a]
Nafion 111 (100% RH)	257	—	67[a]
Nafion 117 (dry)	2.3	9.6	57[b]
Nafion 117 (dry)	2.4	9.2	20[c]
Nafion 112-K (wet)	51.3	—	68[d]
Nafion 112-EDA (wet)	104	—	68[d]
Nafion 117 (75% RH)	160	23	22[e]
Aquivion (75% RH)	120	36	22[e]
Epoxy–amine poly(ionic liquid) (PIL)/IL	100	28	10[f]
PIL/[C2mim][Tf$_2$N]	60	36	69[f]
PIL/IL	105	21	70[f]
Nafion (cast, dry)	1.6	8.9	This work[g]
Nafion + 40 wt% [Bmim][BF$_4$] (dry)	75.4	35.2	This work[g]
Nafion (cast, 100% RH)	209	15.0	This work[h]
Nafion + 40 wt% [Bmim][BF$_4$] (100% RH)	390	29.9	This work[h]

[a] Single-gas permeation test conducted with a feed pressure of 1 atm at 25 °C. [b] Single-gas permeation test conducted with a feed pressure of 2 atm at 35 °C. [c] Single-gas permeation test conducted with a feed pressure of 1 atm 35 °C. [d] Mixed-gas permeation test conducted with a CO_2 partial pressure of 199 kPa at ambient temperature. [e] Single-gas permeation test conducted with a feed pressure of 2 bar at 25 °C, gas permeability data estimated from Fig. 4 and 7 in ref. 19. [f] Single-gas permeation test conducted with a feed pressure of 2 bar at ambient temperature. [g] Single-gas permeation test conducted with a feed pressure of 2 bar at ambient temperature. [h] CO_2/N_2 mixed-gas (10/90 vol%) permeation test conducted with a feed pressure of 2 bar at ambient temperature.
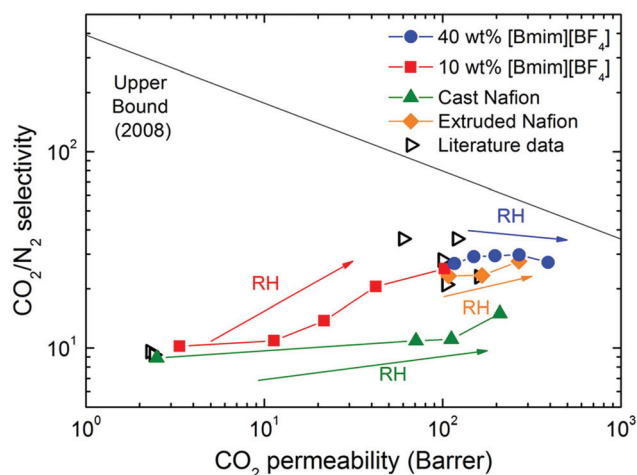

Fig. 14 Robeson plot[@] for the CO_2/N_2 separation performance obtained from mixed-gas permeation tests of Nafion/IL membranes varying in composition (color-coded). Diamonds are literature data from Table 4.

be fabricated with relatively good performance metrics. The results reported in this work reveal that synergy exists between both promoters, suggesting that Nafion membranes can be more fully optimized with regard to their molecular transport properties for CO_2 separation.

4. Conclusions

In the present study, Nafion/IL hybrid membranes containing different IL concentrations have been prepared by physically mixing Nafion solutions with [Bmim][BF$_4$]. The resultant membranes have been physically and chemically characterized, evincing favorable thermal and chemical properties as well as enhanced CO_2 separation performance. While adding 40 wt% [Bmim][BF$_4$] to Nafion yields a CO_2 permeability increase from 1.6 to 75.4 Barrer, the presence of water can further increase the CO_2 permeability to 390 Barrer, which constitutes a 200× enhancement compared to neat Nafion. On the basis of the results reported here, we propose that [Bmim][BF$_4$] in the Nafion/IL hybrid membranes functions as a "first promoter" to improve gas transport for most of the tested species, especially CO_2. Water vapor introduced in the Nafion and Nafion/IL membranes further improve gas permeability as a "second promoter". As the RH increases from 0 to 100%, the CO_2 permeability of the hybrid Nafion/IL membranes increases from 116 to 390 Barrer with no change in CO_2/N_2 selectivity (~30). These observations confirm that synergy exists between the IL and water vapor within the Nafion matrix. The possibility to exploit polyelectrolyte solvent casting as a route to thin separation membranes, without paying a penalty in terms of separation performance, opens new opportunities for the fabrication of Nafion-based CO_2 capture membranes. Judicious incorporation of ILs possessing higher CO_2 solubility and diffusivity into solvent-cast Nafion (by chemisorption of ILs or by preparing blends of chemisorption-/physisorption-introduced ILs), combined with humidified gas streams, might further enhance membrane separation performance. In this regard, a detailed molecular-level investigation of the interactions between hydrated Nafion and ionic additives is clearly warranted.

Conflicts of interest

There are no conflicts to declare.

Acknowledgements

References

1 X. Zhang, X. Zhang, H. Dong, Z. Zhao, S. Zhang and Y. Huang, *Energy Environ. Sci.*, 2012, **5**, 6668–6681.

2 J. Wang, J. Luo, S. Feng, H. Li, Y. Wan and X. Zhang, *Green Energy Environ.*, 2016, **1**, 43–61.

3 P. Li, D. R. Paul and T.-S. Chung, *Green Chem.*, 2012, **14**, 1052–1063.

4 D. L. Gin and R. D. Noble, *Science*, 2011, **332**, 674–676.

5 Z. Dai, L. Ansaloni and L. Deng, *Ind. Eng. Chem. Res.*, 2016, **55**, 5983–5992.

6 Z. D. Dai, R. D. Noble, D. L. Gin, X. P. Zhang and L. Y. Deng, *J. Membr. Sci.*, 2016, **497**, 1–20.

7 J. Deng, L. Bai, S. Zeng, X. Zhang, Y. Nie, L. Deng and S. Zhang, *RSC Adv.*, 2016, **6**, 45184–45192.

8 Z. Dai, L. Bai, K. N. Hval, X. Zhang, S. Zhang and L. Deng, *Sci. China: Chem.*, 2016, **59**, 538–546.

9 S. Raeissi and C. J. Peters, *Green Chem.*, 2009, **11**, 185–192.

10 W. M. McDanel, M. G. Cowan, J. A. Barton, D. L. Gin and R. D. Noble, *Ind. Eng. Chem. Res.*, 2015, **54**, 4396–4406.

11 F. Moghadam, E. Kamio and H. Matsuyama, *J. Membr. Sci.*, 2017, **525**, 290–297.

12 K. Friess, J. C. Jansen, F. Bazzarelli, P. Izak, V. Jarmarova, M. Kacirkova, J. Schauer, G. Clarizia and P. Bernardo, *J. Membr. Sci.*, 2012, **415**, 801–809.

13 Y. Y. Gu, E. L. Cussler and T. P. Lodge, *J. Membr. Sci.*, 2012, **423**, 20–26.

14 T. P. Lodge, *Science*, 2008, **321**, 50–51.

15 J. Y. Yuan, D. Mecerreyes and M. Antonietti, *Prog. Polym. Sci.*, 2013, **38**, 1009–1036.

16 L. Ansaloni, Z. Dai, J. J. Ryan, K. P. Mineart, Q. Yu, K. T. Saud, M.-B. Hägg, R. J. Spontak and L. Deng, *Adv. Mater. Interfaces*, 2017, 1700854.

17 L. Olivieri, H. Aboukeila, M. Giacinti Baschetti, D. Pizzi, L. Merlo and G. C. Sarti, *J. Membr. Sci.*, 2017, **542**, 367–377.

18 Y. Wang, K. S. Chen, J. Mishler, S. C. Cho and X. C. Adroher, *Appl. Energy*, 2011, **88**, 981–1007.

19 C. HeitnerWirguin, *J. Membr. Sci.*, 1996, **120**, 1–33.

20 J. S. Chiou and D. R. Paul, *Ind. Eng. Chem. Res.*, 1988, **27**, 2161–2164.

21 Y. F. Fan, D. Tongren and C. J. Cornelius, *Eur. Polym. J.*, 2014, **50**, 271–278.

22 M. Giacinti Baschetti, M. Minelli, J. Catalano and G. C. Sarti, *Int. J. Hydrogen Energy*, 2013, **38**, 11973–11982.

23 K. A. Mauritz and R. B. Moore, *Chem. Rev.*, 2004, **104**, 4535–4586.

24 F. I. Allen, L. R. Comolli, A. Kusoglu, M. A. Modestino, A. M. Minor and A. Z. Weber, *ACS Macro Lett.*, 2015, **4**, 1–5.

25 A. Kusoglu and A. Z. Weber, *Chem. Rev.*, 2017, **117**, 987–1104.

26 K. Schmidt-Rohr and Q. Chen, *Nat. Mater.*, 2008, **7**, 75–83.

27 S. Yoo, J. Won, S. W. Kang, Y. S. Kang and S. Nagase, *J. Membr. Sci.*, 2010, **363**, 72–79.

28 D. Sun and J. Zhou, *AIChE J.*, 2013, **59**, 2630–2639.

29 K. Broka and P. Ekdunge, *J. Appl. Electrochem.*, 1997, **27**, 117–123.

30 H. Matsuyama, K. Matsui, Y. Kitamura, T. Maki and M. Teramoto, *Sep. Purif. Technol.*, 1999, **17**, 235–241.

31 H. L. Yeager and A. Steck, *J. Electrochem. Soc.*, 1981, **128**, 1880–1884.

32 Y. Wang, H. Chen, Y. Wang, B. Luo, L. Chang, Z. Zhu and B. Li, *Polym. Eng. Sci.*, 2014, **54**, 818–830.

33 D. G. Pye, H. H. Hoehn and M. Panar, *J. Appl. Polym. Sci.*, 1976, **20**, 1921–1931.

34 Z. Dai, L. Ansaloni, D. L. Gin, R. D. Noble and L. Deng, *J. Membr. Sci.*, 2017, **523**, 551–560.

35 Z. Dai and L. Deng, *Int. J. Greenhouse Gas Control*, 2016, **54**(Part 1), 59–69.

36 H. Liu, J. Huang and P. Pendleton, *Energy Procedia*, 2011, **4**, 59–66.

37 B. E. Gurkan, J. C. de la Fuente, E. M. Mindrup, L. E. Ficke, B. F. Goodrich, E. A. Price, W. F. Schneider and J. F. Brennecke, *J. Am. Chem. Soc.*, 2010, **132**, 2116–2117.

38 Z. Lei, C. Dai and B. Chen, *Chem. Rev.*, 2014, **114**, 1289–1326.

39 M. B. Shiflett and A. Yokozeki, *Ind. Eng. Chem. Res.*, 2005, **44**, 4453–4464.

40 M. E. V. Valkenburg, R. L. Vaughn, M. Williams and J. S. Wilkes, *Thermochim. Acta*, 2005, **425**, 181–188.

41 Y. Wang, Y. Kawano, S. R. Aubuchon and R. A. Palmer, *Macromolecules*, 2003, **36**, 1138–1146.

42 S. H. de Almeida and Y. Kawano, *J. Therm. Anal. Calorim.*, 1999, **58**, 569–577.

43 Q. Deng, C. A. Wilkie, R. B. Moore and K. A. Mauritz, *Polymer*, 1998, **39**, 5961–5972.

44 L. G. Lage, P. G. Delgado and Y. Kawano, *J. Therm. Anal. Calorim.*, 2004, **75**, 521–530.

45 Y. Iwai and T. Yamanishi, *Polym. Degrad. Stab.*, 2009, **94**, 679–687.

46 K. Ataka and M. Osawa, *Langmuir*, 1998, **14**, 951–959.

47 J. Schiffer and D. F. Hornig, *J. Chem. Phys.*, 1968, **49**, 4150–4160.

48 Shalu, S. K. Chaurasia, R. K. Singh and S. Chandra, *J. Phys. Chem. B*, 2013, **117**, 897–906.

49 M. Laporta, M. Pegoraro and L. Zanderighi, *Phys. Chem. Chem. Phys.*, 1999, **1**, 4619–4628.

50 J. Ostrowska and A. Narebska, *Colloid Polym. Sci.*, 1984, **262**, 305–310.

51 W. Kujawski, Q. T. Nguyen and J. Néel, *J. Appl. Polym. Sci.*, 1992, **44**, 951–958.

52 N. Nanbu, Y. Sasaki and F. Kitamura, *Electrochem. Commun.*, 2003, **5**, 383–387.

53 J. P. Wu, M. J. Wang and J. P. W. Stark, *J. Quant. Spectrosc. Radiat. Transfer*, 2006, **102**, 228–235.

54 H. G. Haubold, T. Vad, H. Jungbluth and P. Hiller, *Electrochim. Acta*, 2001, **46**, 1559–1563.

55 F. I. Allen, L. R. Comolli, A. Kusoglu, M. A. Modestino, A. M. Minor and A. Z. Weber, *ACS Macro Lett.*, 2015, **4**, 1–5.

56 J. Catalano, T. Myezwa, M. G. De Angelis, M. G. Baschetti and G. C. Sarti, *Int. J. Hydrogen Energy*, 2012, **37**, 6308–6316.

57 M. Mukaddam, E. Litwiller and I. Pinnau, *Macromolecules*, 2016, **49**, 280–286.

58 K. A. Mauritz and R. B. Moore, *Chem. Rev.*, 2004, **104**, 4535–4585.

59 R. M. Barrer and G. Skirrow, *J. Polym. Sci.*, 1948, **3**, 549–563.

60 J. H. Kim, S. Y. Ha and Y. M. Lee, *J. Membr. Sci.*, 2001, **190**, 179–193.

61 N. P. Patel, A. C. Miller and R. J. Spontak, *Adv. Funct. Mater.*, 2004, **14**, 699–707.

62 L. Ansaloni, J. R. Nykaza, Y. Ye, Y. A. Elabd and M. Giacinti Baschetti, *J. Membr. Sci.*, 2015, **487**, 199–208.

63 D. Fu, X. Sun, J. Pu and S. Zhao, *J. Chem. Eng. Data*, 2006, **51**, 371–375.

64 J. Jacquemin, P. Husson, A. A. H. Padua and V. Majer, *Green Chem.*, 2006, **8**, 172–180.

65 P. Feron and A. Jansen, *Sep. Purif. Technol.*, 2002, **27**, 231–242.

66 L. A. Neves, N. Nemestóthy, V. D. Alves, P. Cserjési, K. Bélafi-Bakó and I. M. Coelhoso, *Desalination*, 2009, **240**, 311–315.

67 S. A. Ma, M. Odgaard and E. Skou, *Solid State Ionics*, 2005, **176**, 2923–2927.

68 J. Pellegrino and Y. S. Kang, *J. Membr. Sci.*, 1995, **99**, 163–174.

69 J. E. Bara, D. L. Gin and R. D. Noble, *Ind. Eng. Chem. Res.*, 2008, **47**, 9919–9924.

70 T. K. Carlisle, E. F. Wiesenauer, G. D. Nicodemus, D. L. Gin and R. D. Noble, *Ind. Eng. Chem. Res.*, 2013, **52**, 1023–1032.

71 L. M. Robeson, *J. Membr. Sci.*, 2008, **320**, 390–400.

72 H. B. Park, J. Kamcev, L. M. Robeson, M. Elimelech and B. D. Freeman, *Science*, 2017, **356**, eaab0530.